Radar-Centric ISAC Through Index Modulation: Over-the-air Experimentation and Trade-offs

Murat Temiz, Nial J. Peters, Colin Horne, Matthew A. Ritchie, Christos Masouros
Department of Electronic and Electrical Engineering
University College London (UCL), London, United Kingdom

***Abstract*—This study experimentally demonstrates a radar-centric integrated sensing and communication (ISAC) system that exploits the radar transmission parameters as modulation indexes to communicate with the user devices while performing short-range radar sensing. The center frequency, bandwidth, and polarization of the transmitted radar chirps are used as modulation indexes. The simulation results have been verified by real-time over-the-air experimental measurements that have also revealed the trade-off between the radar sensing performance and communication data rate, depending on the radar waveform parameters selected in the ISAC system. The proposed dual-function radar and communication system was shown to reach up to 10 Megabits/s throughput depending on the bandwidth and centre frequency separations and chirp duration.**

***Index Terms*—index modulation, integrated sensing and communication, radar sensing, wireless communication**

I. Introduction

The frequency spectrum is becoming increasingly more congested and contested due to rapidly increasing bandwidth of radar sensing and communication systems [1]. The integrated sensing and communication (ISAC) systems that utilize the same frequency resources for both operations are seen as key solutions for the congested frequency spectrum problem. ISAC systems can be designed as *Radar-Centric* or *Communication-Centric* systems [2]. In the *Radar-Centric* ISAC systems, the communication data is embedded in radar signals [3], while *Communication-Centric* ISAC solutions exploit the communication signals for radar sensing [4]. In this study, we have designed, implemented and demonstrated a Radar-Centric ISAC system that enables communication functions in short-range radar systems through index modulation (IM) within frequency-modulated continuous-wave (FMCW) radar chirps.

The IM exploits various waveform features as modulation indexes to modulate communication data [5]. For example, selections of antennas, subcarriers, time slots or other signal features can be exploited as indexes [6]. IM does not require special waveform types and may be implemented without significantly changing the signals, hence it has been recently considered to modulate communication data within radar waveforms [7]–[13]. For instance, Huang *et. al* proposed multi-carrier agile joint radar-communication (MAJoRCom) system which jointly utilize the antenna and carrier frequency selections of radar waveforms to modulate data [7]. Moreover, Ma *et. al* proposed a method that works with FMCW signals [9], which makes use of the active antenna index and carrier frequency selection of the FMCW signals to convey data to the users. In the aforementioned IM-based ISAC studies [7]–[13], it is usually assumed that the channel state information (CSI) is perfectly known by the communication receivers, hence it is possible to take advantage of multiple antennas and phase diversity as IM indexes because they can be decoded using the CSI. However, the CSI may not be accurately estimated owing to the nature of wideband radar waveforms, thus such ideas are difficult to implement in real-time ISAC systems where the channel might change rapidly, making the CSI estimation challenging using radar waveforms. Consequently, we investigate the use of the polarization of the radar signals as an IM index, which is easier to estimate than the antenna selection index at the receiver node. The polarizations of the received signals can be estimated at the receiver without requiring a precise CSI, thanks to the polarization diversity. The proposed ISAC method makes use of continuous waveforms (i.e., FMCW), hence it can be used in self-driving vehicles or other short-range sensing applications.

This study proposes and demonstrates a radar-centric ISAC approach through IM to transmit data without significantly affecting the radar performance. The features of the FMCW chirps are utilized as IM indexes to convey data within chirps at relatively high data rates. Making use of both vertical (V-pol) and horizontal (H-pol) polarizations for radar sensing also enables the radar to acquire more information about the targets because some target features may be better acquired in one specific polarization and dual-polarized radar may also provide a higher SNR [14]. The UCL ARESTOR platform [15] was used as the experimental platform to verify the proposed ISAC concept. The ISAC transmitter was implemented on one ARESTOR platform to transmit modulated FMCW chirps and the second ARESTOR platform was used to receive the chirps and decode the received data. The ISAC setup was tested in field trials with moving and static targets. The proposed method provides a low hardware complexity ISAC architecture because it does not need multiple antennas and CSI. Moreover, only a single digital block, RF chain and dual-polarized antenna are sufficient to transmit ISAC waveforms.

The contributions of this study are summarized as:

- This study proposes a novel IM-based ISAC architecture by making use of a dual-polarized antenna. In the previous studies, polarization is not considered as an index.
- This study experimentally shows the trade-offs between the radar sensing performance and communication data rate depending on the radar waveform parameters.

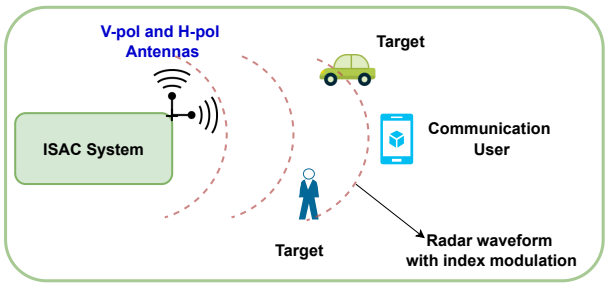

Fig. 1: IM-based FMCW ISAC system.

II. System Model

The proposed ISAC system employs the features of FMCW chirps as IM indexes to convey communication data while carrying out short-range radar sensing as the primary function as shown in Fig 1. The bandwidth (BW), polarization (P), and carrier frequency (f_c), of the FMCW chirps are used as indexes to modulate the communications data. An FMCW chirp is given by

$$u(t) = Ae^{-j\pi\left(2f_c t+\rho t^2\right)}, \quad t \in [0, T_c], \tag{1}$$

where $A(t)$, f_c and T_c are the amplitude, carrier frequency and the sweep duration of a chirp, respectively. Moreover, $\rho = BW/T_c$ is the slope of the chirp with BW being the bandwidth of the chirp. The chirps are transmitted either in V-pol, H-pol or both (V-pol and H-pol) antennas. Accordingly, the transmitted nth signal consisting of chirps in V-pol and H-pol with IM indexes is given by

$$\begin{aligned} X_n &= u_n^V(t) + u_n^H(t) \\ &= A^V e^{-j\pi(2f_c^V t+BW^V/T_c t^2)} \\ &+ A^H e^{-j\pi(2f_c^H t+BW^H/T_c t^2)}, \end{aligned} \tag{2}$$

where $t \in [0, T_c]$, and superscript V and H denote the polarizations of the modulation indexes A, f_c and BW. Moreover, $A^V \in \{0, 1\}$ and $A^H \in \{0, 1\}$ indicate if a chirp is transmitted in the corresponding polarization during the nth transmission, resulting in the polarization index $p_n = \{V, H, VH\}$.

A. Radar Signal Processing and Target Detection

The radar signals reflected from the targets are processed via standard FMCW radar processing techniques [16]. The processing starts with mixing the return signal with a replica of the transmitted signal. The result of the mixing process is a *beat* signal, and its frequency indicates the range of the target the return has been reflected from, and it can be estimated by spectral analysis. The spectral analysis is carried out in the ARESTOR hardware. Details of the ARESTOR FMCW radar implementation can be found in [17].

B. Communication Data Modulation

The bandwidth, carrier centre frequency and polarization of the chirps are used as IM indexes for data modulation.

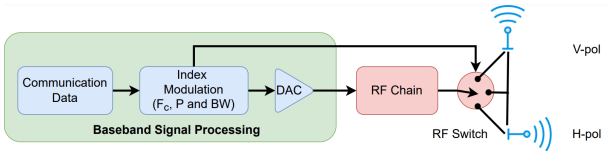

Fig. 2: IM-based ISAC transmitter architecture.

Assuming that the carrier frequency f_c of the chirps is varied by Δ_f steps between $f_{(min)}$ and $f_{(max)}$ as

$$f_{(min)} \leq f_{(min)} + k\Delta_f \leq f_{(max)}, \tag{3}$$

where $k = 0, 1, ..., K-1$ denotes the index of the carrier starting frequency and K is the total number of center frequency indexes, hence, $f_c = f_{(min)} + k\Delta_f$. The set of bandwidth options for the chirps is defined as

$$BW_{(min)} \leq BW_{(min)} + l\Delta_{BW} \leq BW_{(max)}, \tag{4}$$

where $BW_{(min)}$, $BW_{(max)}$, Δ_{BW} and $l = 0, 1, ..., L-1$ are the minimum bandwidth, maximum bandwidth, bandwidth spacing and bandwidth index and L is the number of bandwidth indexes, and the bandwidth of the chirp is $BW = BW_{(min)} + l\Delta_{BW}$. Only three polarization states are considered, namely only vertical (V), only horizontal (H) polarizations or both (VH), therefore, the number of polarization indexes is $P = 3$.

C. ISAC Transmitter Architecture

In addition to the dual-polarized transmit antenna, the radar node is also equipped with a dual-polarized radar receive antenna to simultaneously receive radar returns for radar sensing. The radar waveform is transmitted either in the V-pol, H-pol or in both polarizations during each chirp duration. The transmitter architecture employed at the radar node is shown in Fig. 2, where a single digital block and RF chain are utilized to serve both V-pol and H-pol channels using an RF switch that switches between V-pol and H-pol. Assuming that L bandwidth, K centre frequency, and three polarization (V, H, VH) options are available, then the number of bits can be transmitted in each chirp duration by the proposed IM is given by,

$$N_{bits} = \lfloor \log_2(3KL) \rfloor \tag{5}$$

where $\lfloor . \rfloor$ is the floor function. Furthermore, the communication throughput of the ISAC system is given by

$$R_{com} = \frac{1}{T_c} N_{bits}(1-\gamma), \tag{6}$$

where T_c and γ denote the chirp duration and symbol error rate (SER), respectively.

D. Communication Receiver Architecture

During the nth transmission, the signals received at the communication receiver in V-pol and H-pol are given by

$$S_n^V(t) = u_n^V(t) * h^V(t) + u_n^H(t) * h^{HV}(t) + n^V(t), \tag{7}$$

$$S_n^H(t) = u_n^H(t) * h^H(t) + u_n^V(t) * h^{VH}(t) + n^H(t), \tag{8}$$

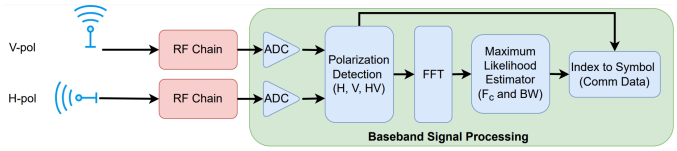

Fig. 3: IM-based ISAC receiver architecture.

where $*$ indicates the convolution operation, $u_n^V(t)$ and $u_n^H(t)$ denote the chirps transmitted in V-pol and H-pol channels as given by (2). Moreover, $h^V(t)$ and $h^H(t)$ denote the V-pol and H-pol channels between the ISAC transmitter and communication receiver, and $h^{HV}(t)$ and $h^{VH}(t)$ denote the polarization leakage channels between the V-pol and H-pol antennas. In addition, $n^V(t)$ and $n^H(t)$ denote the complex-valued additive white Gaussian noise (AWGN) with zero mean and variance σ_n^2 as $\mathcal{CN}\left(0, \sigma_n^2\right)$ in the V-pol and H-pol at the receiver, respectively.

The proposed communication receiver has a two-stage architecture as shown in Fig.3. In the first stage, the polarization of the received chirp is estimated by comparing the received signals in H-pol and V-pol channels to a threshold. The threshold of the polarization detector, T_{pol}, is determined as

$$T_{pol} = \sigma_n^2 + p_{sig}/\beta + \alpha_{pol}^2, \tag{9}$$

where σ_n^2 is the noise variance and β is a coefficient that needs to be optimally selected with regard to the polarization leakage α_{pol} and noise variance σ_n^2. After estimating the polarization of the received signal as $\hat{p}_n \in \{V, H, VH\}$, the received chirp $S_n(t) \in \{S_n^V(t),\ S_n^H(t)\}$ during the nth transmission is transformed into the frequency domain using the Fourier transform as

$$W_n = \int_{-\infty}^{\infty} S_n(t) e^{-j2\pi ft} dt, \tag{10}$$

where $0 \leq t \leq T_c$ for each chirp. The fast Fourier transform (FFT) is used to perform Fourier transform. After FFT, the received signals are normalized before estimating the bandwidth and center frequency indexes.

In the second stage, the bandwidth and the center frequency indexes of the received chirps are estimated using a maximum likelihood estimator. This is expressed as

$$\underset{(\hat{k}_n, \hat{l}_n)}{\arg\min} \quad ||W_n - \mathcal{F}||_2, \tag{11}$$

where $\mathcal{F} = \{W_{(1,1)}, \cdots W_{(k,l)}, \cdots, W_{(K,L)}\}$ is the set of chirps (i.e., code-book) consisting of all possible bandwidth and center frequency combinations, and $||.||_2$ denotes the L_2 norm. Furthermore, W_n is the nth received radar chirp in the frequency domain and $(\hat{k}_n, \hat{l}_n)$ is the estimated centre frequency and bandwidth indexes of the nth radar chirp. Including the estimated polarization index $(\hat{p}_n)$, the indexes of the nth chirp are estimated as $(\hat{p}_n, \hat{k}_n, \hat{l}_n)$ and then these indexes are decoded to the corresponding communication symbol.

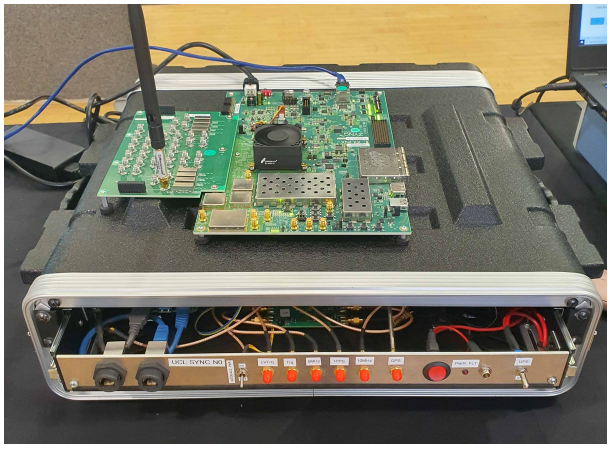

Fig. 4: UCL ARESTOR Multifunction RF Platform

III. ARESTOR RF Sensor Hardware Platform

The hardware used in experimental measurements was the UCL ARESTOR platform [15]. ARESTOR is a Radio Frequency System on Chip (RFSoC) [18] system based on the Xilinx ZCU111 as shown Fig.4. The ARESTOR platform has been developed at UCL to provide a flexible, highly configurable RF sensor that is capable of operating in multiple sensing modes. These modes might be operated serially by reconfiguring the device as necessary on-the-fly, or multiple modes can be operated in parallel. For instance, ARESTOR can be used an FMCW active radar concurrently operating with a passive radar implementation in different frequency bands [17]. The characteristics of the RFSoC device used on the ARESTOR are shown in Table I. Additionally, ARESTOR has been equipped with 32 GB DDR RAM.

TABLE I: Features of ARESTOR RFSoC

No of DAC / ADC Bits	14 / 12-bit
No of channels DAC / ADC	8 / 8
ADC Sample Rate	4.096 GSPS
DAC Sample Rate	6.554 GSPS
System Logic Cells (K)	930
System Memory (MB)	60.5
DSP Slices	4272
Processors	Arm Cortex-A53 + Arm Cortex-R5

In addition to the high-speed hardware architecture, the ARESTOR platform consists of an ecosystem which provides in-built tools, written in Python, which automatically configure and build the design elements to form the final desired system. The ARESTOR ecosystem consists of a number of standard modules which may be connected together to form the desired radar blocks such as the signal de-ramping process and decimation blocks. This paper presents the first published results of the use of the ARESTOR platform for ISAC applications.

IV. Experimental Set-up

The measurement setup is shown in Fig. 5, where dual-polarized radar transmit antenna, communication receive an-

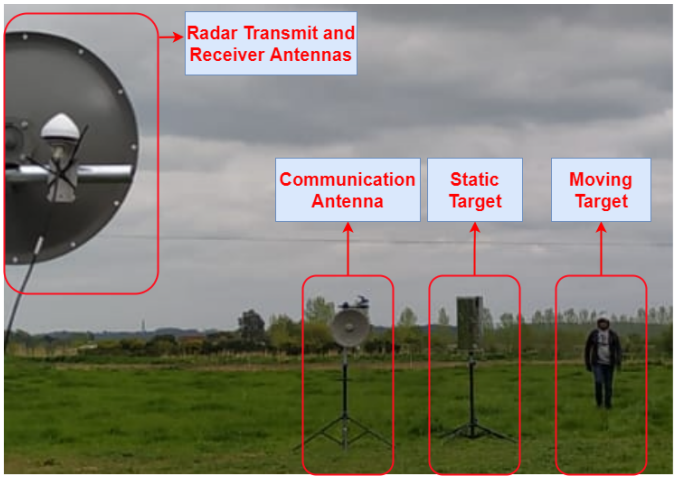

Fig. 5: Field trials of the proposed architecture.

TABLE II: The number of bits transmitted per radar chirp within 2.4 GHz ISM band with different ΔBW and Δf values.

ΔBW	Δf	N_{cons}	N_{bits}
5 MHz	5 MHz	$3 * 30$	6 bits
2 MHz	2 MHz	$3 * 126$	8 bits
2 MHz	1 MHz	$3 * 245$	9 bits

tenna, static and moving targets are presented. The moving target was walking towards the radar and away from the radar during measurements. Two ARESTOR platforms, shown in Fig 4, were used in measurements. The first one was used as a ISAC node to perform radar sensing and transmit communication data, and the second ARESTOR platform was used as the communication receiver. Experimental measurements were conducted in a farm to avoid interference from other RF transmitters in 2.4 GHz ISM (industrial, scientific, and medical) band. Moreover, open field measurements provides line-of-sight dominant links which are generally desired for radar measurements.

Two synchronised FMCW processing chains were implemented in the ARESTOR to provide the V-pol and H-pol channels at the ISAC node. Another two separate processing chains were implemented for the dual-pol captures at the communication receiver node. The proposed ISAC system is designed to operate in 2.4 GHz ISM band, accordingly, the generated waveforms must be entirely within this ISM band, i.e. between 2400 MHz to 2483.5 MHz [19]. Moreover, the bandwidth of the transmitted radar chirps were between 40 MHz and 55 MHz. Consequently, the number of waveforms in the code-book are restricted by the centre frequency spacing (Δf) and bandwidth spacing (ΔBW) owing to these frequency spectrum limitations. Table II presents the experimentally tested waveform bandwidth spacing, centre frequency spacing and channel (dual or single) combinations and resulting modulation constellation size (N_{cons}) and corresponding number of bits (N_{bits}) that can be transmitted within in each radar chirp.

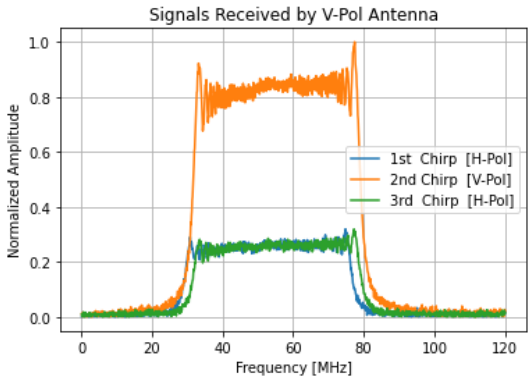

(a) V-pol receiver

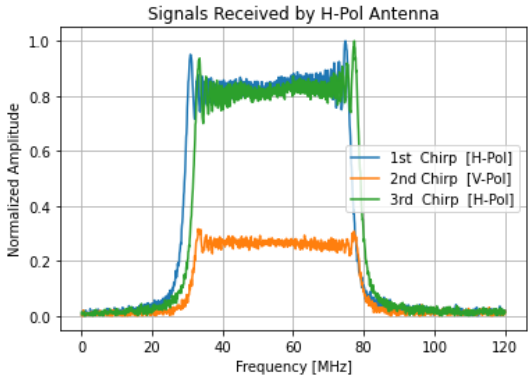

(b) H-pol receiver

Fig. 6: Example signals received by V-pol and H-pol communication antennas.

V. Simulation and Experimental Results

In this section, the communication data rate and radar sensing performance of the proposed ISAC system have been evaluated via simulations and real-time over-the-air experimental measurements performed using the ARESTOR platform [15]. Fig. 6 shows the example signals received at V-pol and H-pol communication antennas when three different index-modulated chirps are transmitted by the dual-polarized ISAC antennas. In this example, the 1st and 3rd chirps are transmitted by the H-pol ISAC antenna while the 2nd chirp is transmitted by the V-pol ISAC antenna. The signals received at communication V-pol and H-pol channels are clearly seen and their centre frequency and bandwidth indexes can be estimated by the proposed receiver architecture. Moreover, a polarization leakage between the antennas is observed, which is anticipated as the polarization of the antennas are not perfect and there might be a misalignment between the transmit and receive antennas, causing some level of polarization leakage. This polarization leakage is also modeled in simulations using the channel model given by (7) and (8).

The proposed ISAC platform has been evaluated by simulations and experimental measurements performed in the scenario illustrated in Fig. 5 in a farm to avoid possible interference from other devices operating in 2.4 GHz ISM

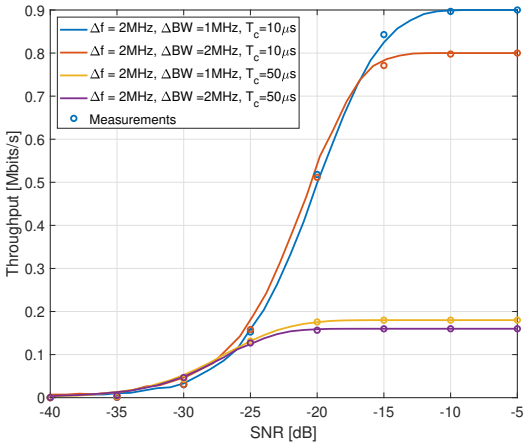

Fig. 7: Measured and simulated throughput of the proposed ISAC system.

band. Fig. 7 illustrates the measured and simulated throughput of the received communication data. These results have shown that the ISAC system delivers a reliable data communication even in very low SNR values. Experimental measurements and simulations results showed a good agreement and they have proved that the proposed ISAC architecture can work even with -10 dB SNR at the communication receiver. This provides a significant improvement compared to the previous studies such as [9], where higher SNR is required for communication.

Reducing the chirp duration allows the ISAC system to achieve a higher throughput as shown in Fig. 7, however this is at the expense of radar performance as observed in Fig. 8. Fig. 8 presents the radar range image of the static and moving targets from V and H polarized antennas from experimental measurements. Both targets are clearly observed in Fig. 8a, b, and c ($T_c = 100$ μs and $T_c = 50$ μs) although there are some fluctuations that are mainly caused by the varying bandwidth of the FMCW chirps. Fig. 8c and d show example radar range images obtained from V polarized antenna with $T_c = 10$ μs and $T_c = 50$ μs chirp duration, respectively. [1] Fig. 8 shows that when $T_c = 100$ μs or $T_c = 50$ μs both static and moving targets can be detected and their ranges can be estimated. On the other hand, when $T_c = 10$ μs, the shorter range static target is still detectable, but the detection of the moving target becomes more challenging as its range increases. Shorter chirp length results in reduced SNR as well as impacting the maximum radar range in the implemented FMCW radar due to filtering effects of the radar receiver.

The trade-off between the radar sensing performance and communication throughput is illustrated in Fig. 9, where the chirp duration (T_c) causing a trade-off between the communication and radar. Shorter chirp duration allows the ISAC system to transmit data at higher throughputs (i.e., up to 10 Megabits/s) while it causes a decrease in the radar SNR.

[1]The H-pol radar images are not shown for $T_c = 10$ μs and $T_c = 50$ μs for the sake of brevity as it is given for $T_c = 100$ μs.

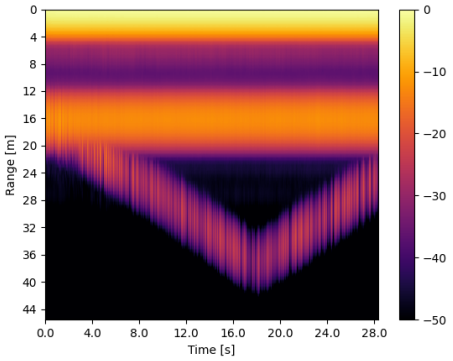

(a) V-pol Radar Image with $T_c = 100$ μs.

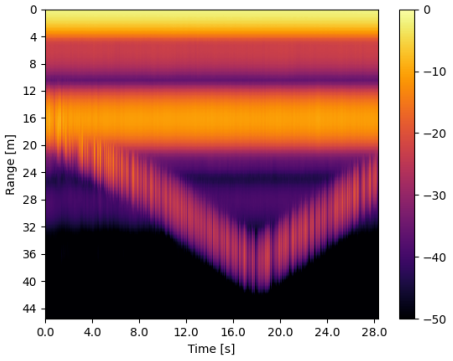

(b) H-pol Radar Image with $T_c = 100$ μs.

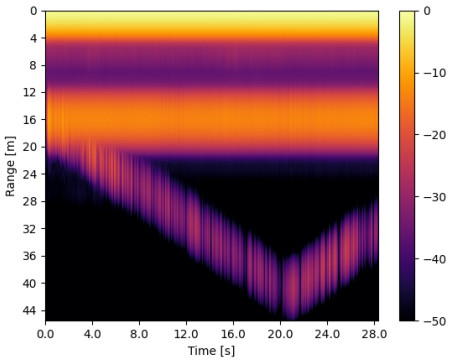

(c) V-pol Radar image with $T_c = 50$ μs.

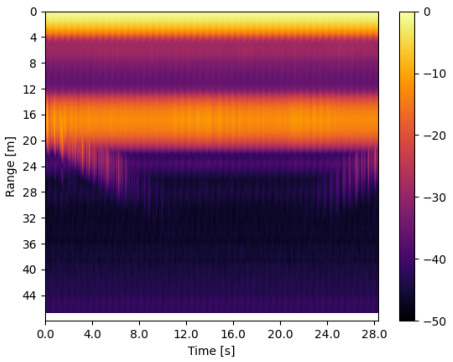

(d) V-pol Radar image with $T_c = 10$ μs.

Fig. 8: V-pol and H-pol range images.

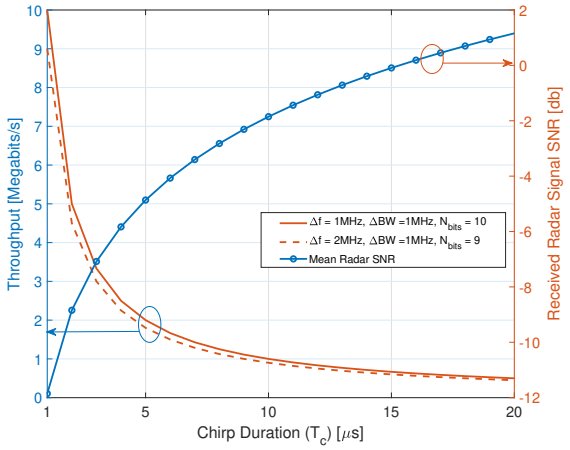

Fig. 9: The trade-off between radar and communications.

However, this trade-off does not consider integrating multiple chirps, which is expected to improve the radar sensing performance when shorter chirps are employed by integrating multiple of them for radar sensing. This will be investigated in future studies. These simulation and measurement results have shown a good agreement and given an insight into the performance of the proposed ISAC system. Moreover, measurements also were also used to experimentally evaluate the radar sensing performance. Depending on the application, a suitable chirp duration can be chosen to satisfy the radar and communication requirements of the application. For instance, if it aims to detect a large target –resulting in high SNR radar returns– then a short chirp duration can be selected to increase the communication data rate.

VI. Conclusion

This study has proposed a radar-centric FMCW ISAC system with low hardware complexity, and evaluated its communication and radar sensing performance by both simulations and experimental measurements. Making use of bandwidth, centre frequency and polarization of the chirps as indexes, communication throughputs of up to a 10 Megabits/s is achieved. This study has also experimentally demonstrated the trade-off between the communication data rate and radar performance, which is caused by chirps parameters. Future research will aim to improve the communication and radar performance by enabling both polarization channels at the same time and investigate radar signal processing techniques to mitigate the impact of the varying chirp parameters on the radar sensing.

Acknowledgment

The authors would like to thank the Defence and Security Accelerator (DASA) for the funding that supported this research. The authors would also like to thank D. Dhulashia and P. Beasley for their help with field trials and measurements.

References

[1] F. Liu, C. Masouros, A. P. Petropulu, H. Griffiths, and L. Hanzo, "Joint radar and communication design: Applications, state-of-the-art, and the road ahead," *IEEE Transactions on Communications*, vol. 68, no. 6, pp. 3834–3862, June 2020.

[2] F. Liu, Y. Cui, C. Masouros, J. Xu, T. X. Han, Y. C. Eldar, and S. Buzzi, "Integrated sensing and communications: Toward dual-functional wireless networks for 6G and beyond," *IEEE Journal on Selected Areas in Communications*, vol. 40, no. 6, pp. 1728–1767, June 2022.

[3] S. D. Blunt, P. Yatham, and J. Stiles, "Intrapulse radar-embedded communications," *IEEE Transactions on Aerospace and Electronic Systems*, vol. 46, no. 3, pp. 1185–1200, July 2010.

[4] C. Baquero Barneto, T. Riihonen, M. Turunen, L. Anttila, M. Fleischer, K. Stadius, J. Ryynänen, and M. Valkama, "Full-duplex OFDM radar with LTE and 5G NR waveforms: Challenges, solutions, and measurements," *IEEE Transactions on Microwave Theory and Techniques*, vol. 67, no. 10, pp. 4042–4054, Oct 2019.

[5] E. Basar, M. Wen, R. Mesleh, M. Di Renzo, Y. Xiao, and H. Haas, "Index modulation techniques for next-generation wireless networks," *IEEE Access*, vol. 5, pp. 16 693–16 746, 2017.

[6] T. Mao, Q. Wang, Z. Wang, and S. Chen, "Novel index modulation techniques: A survey," *IEEE Communications Surveys Tutorials*, vol. 21, no. 1, pp. 315–348, Firstquarter 2019.

[7] T. Huang, N. Shlezinger, X. Xu, Y. Liu, and Y. C. Eldar, "MAJoRCom: a dual-function radar communication system using index modulation," *IEEE Transactions on Signal Processing*, vol. 68, pp. 3423–3438, 2020.

[8] A. Şahin, S. S. M. Hoque, and C.-Y. Chen, "Index modulation with circularly-shifted chirps for dual-function radar and communications," *IEEE Transactions on Wireless Communications*, pp. 1–1, 2021.

[9] D. Ma, N. Shlezinger, T. Huang, Y. Liu, and Y. C. Eldar, "FRaC: FMCW-based joint radar-communications system via index modulation," *IEEE Journal of Selected Topics in Signal Processing*, vol. 15, no. 6, pp. 1348–1364, Nov 2021.

[10] L. Giroto de Oliveira, B. Nuss, M. B. Alabd, A. Diewald, M. Pauli, and T. Zwick, "Joint radar-communication systems: Modulation schemes and system design," *IEEE Transactions on Microwave Theory and Techniques*, vol. 70, no. 3, pp. 1521–1551, March 2022.

[11] W. Baxter, E. Aboutanios, and A. Hassanien, "Joint radar and communications for frequency-hopped MIMO systems," *IEEE Transactions on Signal Processing*, vol. 70, pp. 729–742, 2022.

[12] D. Ma, N. Shlezinger, T. Huang, Y. Shavit, M. Namer, Y. Liu, and Y. C. Eldar, "Spatial modulation for joint radar-communications systems: Design, analysis, and hardware prototype," *IEEE Transactions on Vehicular Technology*, vol. 70, no. 3, pp. 2283–2298, March 2021.

[13] G. Huang, Y. Ding, S. Ouyang, and V. Fusco, "Index modulation for OFDM RadCom systems," *The Journal of Engineering*, vol. 2021, no. 2, pp. 61–72.

[14] M. Conti, C. Moscardini, and A. Capria, "Dual-polarization DVB-T passive radar: Experimental results," in *2016 IEEE Radar Conference (RadarConf)*, May 2016, pp. 1–5.

[15] N. Peters, C. Horne, and M. A. Ritchie, "Arestor: A multi-role RF sensor based on the Xilinx RFSoC," in *2021 18th European Radar Conference (EuRAD)*, April 2022, pp. 102–105.

[16] H. Griffiths, "New ideas in FM radar," *Electronics & Communications Engineering Journal*, vol. 2, no. 5, p. 185, 1990.

[17] M. A. Ritchie, N. Peters, and C. Horne, "Joint Active Passive Sensing using a Radio Frequency System-on-a-Chip Based Sensor," in *International Radar Symposium (IRS) 2022*, 2022.

[18] Xilinx, "Zynq UltraScale+ RFSoC." [Online]. Available: https://www.xilinx.com/products/silicon-devices/soc/rfsoc.html

[19] Ofcom, "UK radio interface requirement for wideband transmission systems operating in the 2.4 ghz ISM band," Jan 2018.